Experimental and Model Investigation on Radar Classification Capability

Paolo Ferrazzoli, *Member, IEEE*, Leila Guerriero, and Giovanni Schiavon

***Abstract*—The capability of multifrequency polarimetric synthetic aperture radar (SAR) to discriminate among nine vegetation classes is shown using both experimental data and model simulations. The experimental data were collected by the multifrequency polarimetric AIRSAR at the Dutch Flevoland site and the Italian Montespertoli site. Simulations are carried out using an electromagnetic model, developed at Tor Vergata University, Rome, Italy, which computes microwave vegetation scattering. The classes have been defined on the basis of geometrical differences among vegetation species, leading to different polarimetric signatures. It is demonstrated that, for each class, there are some combinations of frequencies and polarizations producing a significant separability. On the basis of this background, a simple, hierarchical parallelepiped algorithm is proposed.**

***Index Terms*—Classification, modeling, radar polarimetry, synthetic aperture radar, vegetation mapping.**

I. Introduction

In RECENT years, several experiments have been carried out to investigate the potential of synthetic aperture radar (SAR) in remote sensing of vegetation. Airborne radars have overflown several sites worldwide, while ERS-1, ERS-2, and JERS-1 satellites have collected multitemporal data on a continuous basis. Some important goals of these experimental activities are the classification among different land categories and the retrieval of important physical parameters, such as vegetation biomass and soil moisture.

A considerable amount of radar signatures is now available, and the development of reliable algorithms, aimed at classifying and retrieving parameters, is in progress. Indeed, the two objectives are not independent. In fact, the radar sensitivity to biomass depends on the vegetation elements geometry, while the discrimination capability is improved when the plant is well developed, or when the whole crop cycle is covered by multitemporal data.

A considerable amount of statistical classification research has been carried out, indicating that SAR systems have a good capability in discriminating among various classes over agricultural and forest sites. A critical review of significant results is reported in [1]. In general, classification results are poor if only single-frequency, single-polarization, single-overpass data are available, unless broad categories are defined (such as urban, forest, agricultural, water). In order to improve the radar classification capability, either multitemporal or multifrequency/multipolarization data are required. Multitemporal data, which may be achieved by satellite systems, are particularly important to separate among agricultural crops, using the temporal differences in the crop development cycles. Multifrequency/multipolarization data are made available by some airborne SAR systems, such as AIRSAR and E-SAR. These systems may acquire interesting classification results even in the case of single flight, due to differences in multifrequency polarimetric features associated to different plant geometries.

Previous papers [1], [2] indicate that a statistically valid classification algorithm must be accompanied by a good knowledge of the interactions between electromagnetic waves and vegetation elements of various density, shape, dimensions, and orientations. Theoretical electromagnetic models are useful to this scope. In fact, the experimental backscatter differences among classes may be associated to differences in plant geometry by means of model simulations; this improves the reliability of the observed separations. Therefore, when an algorithm tested on a site is validated by model simulations, confidence may be placed on the achievement of valid results in other sites as well. After validations over various sites are carried out, reliable classification results should be obtained, even reducing in the dimensions of the training set.

A well-known algorithm based on electromagnetic modeling was proposed in [2], where three classes were defined: surface, dihedral elements, and thick vegetation. When applied to experimental data collected by the L-band Jet Propulsion Laboratory (JPL) polarimeter, the algorithm allowed the researchers to correctly interpret several image properties. Another model-based algorithm was proposed in [3] and applied to polarimetric radar data collected at P-, L-, and C-band. The algorithm classified among eight general categories: no vegetation, low vegetation, dihedral low vegetation, medium vegetation, dihedral medium vegetation, regular forest, dihedral regular forest, and urban. In [1], a knowledge-based algorithm classified among urban, surface, short vegetation and three kinds of forest using ERS-1 and JERS-1 data.

In this paper, the SAR discrimination capability is investigated by analyzing the experimental data collected by the polarimetric AIRSAR at the Dutch Flevoland site (MAESTRO-1 experiment, 1989) and at the Italian Montespertoli site (MAC-Europe experiment, 1991). Nine classes, corresponding to vegetation present in at least one site, are considered. The experimental data are interpreted with the aid of the microwave vegetation model developed at

Manuscript received May 4, 1998. This work was supported in part by ASI, Agenzia Spaziale Italiana.

The authors are with the Dipartimento di Informatica, Sistemi e Produzione, Università Tor Vergata–Ingegneria, I-00133 Rome, Italy (e-mail: schiavon@disp.uniroma2.it).

Publisher Item Identifier S 0196-2892(99)01177-8.

Tor Vergata University [4], [5], Rome, Italy. For each class, experimental data and model simulations are shown. Both of them indicate that, for some combinations of frequency and polarization, each class shows a behavior appreciably different from that of the others. This ensures a reliable classification capability. On the basis of this analysis, a simple hierarchical scheme is proposed.

II. Materials and Methods

A. Experimental Data

The experimental data used in this paper were collected over forests and agricultural fields by AIRSAR, which is a fully polarimetric radar operating at P- (0.45 GHz), L- (1.2 GHz), and C-band (5.3 GHz) [6]. In particular, the AIRSAR data obtained over the Dutch Flevoland site in summer 1989 and over the Italian Montespertoli site in summer 1991 are used. The analysis is based on the polarized backscatter coefficient σ° measured at P-, L-, and C-band and at HH-, HV-, VV-, RR- (circular copolar), RL- (circular cross polar), 45C- (45° copolar), 45X-polarization (45° crosspolar), for a total of 21 features (3 frequencies $\times$ 7 polarizations). To indicate the combinations of bands and polarizations, the $\sigma^\circ_{\mathrm{FPQ}}$ symbol (FPQ in the figures), is used: the first character (F) indicates the band (P, L, or C), while the other characters indicate the polarization (HH, HV, VV, RR, RL, 45C, or 45X).

The available SAR data were in slant range. For each pixel, the calibrated backscatter coefficient has been computed using corner reflectors, as described in [7] (for Flevoland data) and in [8] (for Montespertoli data). The calibration accuracy is estimated to be ± 1 dB. The resolution is 12 m in azimuth and 6.66 m in range. The number of looks is four for Flevoland data and 16 for Montespertoli data. The number of pixels per field ranges from about 100 for some small fields at Montespertoli to several thousands for some very large Dutch fields. As will be discussed in Section IV, a good classification accuracy is achieved when field averages are considered, i.e., when a sample is obtained by averaging the σ°'s of all pixels belonging to a given field. Averages have been computed also over nine pixels areas (3 pixels in azimuth $\times$ 3 pixels in range). As expected, the classification accuracy is partially degraded in this latter case, but it remains significant (see results of Section IV).

The Flevoland data were collected in the framework of the MAESTRO-1 campaign [9]. The fields were observed by AIRSAR on August 16, 1989, with an incidence angle ranging between $\sim$40° and $\sim$50°. The results were made available to many researchers. The Flevopolder subarea of the Flevoland site, which included agricultural fields of various species, has been considered. Seventeen fields of potato, 16 fields of sugarbeet, five fields of corn, three fields of alfalfa, and 12 bare soil fields have been selected. Extensive surveys and intensive ground measurements over some fields were carried out in the area. Survey results are published in [10], while further field information has been extracted from [11] or has been directly made available to us by University of Wageningen. In general, sugarbeet and potato fields were healthy and well developed, with a moisture content of $\sim$90%. Corn fields were senescent, and in most of the cases, leaves had been severely damaged by a hailstorm. Bare soils were generally moist (with a volumetric soil moisture content higher than 30%) and showed a wide variability in their roughness. No detailed alfalfa ground data were available. The variability of backscattering parameters has been analyzed, and it has been verified that the effects of the incidence angle variation (between $\sim$40° and $\sim$50°) are negligible with respect to those due to variations of plant properties.

The Montespertoli data were collected in the framework of the MAC-Europe 91 campaign [12]. The site was observed three times (June 22, June 29, July 14) and at three incidence angles (20, 35, and 50°). Data obtained at 50° are considered in this paper because they are more suitable to be joined with MAESTRO-1 signatures. Moreover, only the first two flights are considered since 50° data of the third flight were partially corrupted. The site is generally hilly, but it includes a flat region where agricultural fields, small forests, and olive groves are present. Detailed information about the site is available in [8] and [13]. The considered areas include seven forests, eight olive groves, four fields of sunflower, three fields of sorghum, one field of corn, two fields of colza, 11 fields of wheat, three fields of alfalfa, and three bare soil fields.

Forests were dominated by oak species and were dense, with basal areas (i.e., normalized trunk base areas) in the range 70–150 m^2/ha, trunk densities in the range 2000–8000 ha^{-1}, and tree heights in the range 10–20 m. Olive groves basal areas were $\sim$10 m^2/ha for all selected fields, densities were $\sim$300 ha^{-1}, and tree heights were $\sim$3 m.

For some crops, such as sunflower, corn, alfalfa, and sorghum, the radar measurements were carried out on different crop conditions. The range of variations of the plant water content (in $\mathrm{kg/m}^2$) was $\sim$0.5–5.0 for sunflower, $\sim$0.2–1.5 for corn, $\sim$0.2–1.0 for sorghum and $\sim$0.2–3.0 for alfalfa. The moisture content was 85–90% for corn, sorghum, and sunflower, while it was 80–85% for alfalfa. Wheat and colza fields were in the ripening stage. The plant density of sunflower and corn was <10 m^{-2}; these crops were characterized by large vertical stalks (stalk diameter $=$ 1–3 cm), and wide leaves (average leaf area $=$ 10–40 cm^2). The plant density of colza, wheat, and alfalfa was in the range 80–500 m^{-2}; these crops were characterized by small vertical stalks (stalk diameter $=0.2$–1.5 cm), while leaves were small (<1 cm^2) or absent.

B. Definition of Classes

The vegetation samples that were present in the two sites have been subdivided into nine classes, adopting the following hierarchical scheme.

- First of all, the well-established subdivision among surface scattering (bare soils), dihedral scattering (senescent and partially defoliated corn), and volume scattering (other vegetation species) [2] has been applied.
- Within the classes, where volume scattering is significant, the subdivision described in [13], based on the number of plants per m^2 (N), has been adopted. The N

TABLE I
CLASS DEFINITION

Vegetation type	Biomass (kg/m^2)			
	0 - 2	2 - 4	4 - 10	> 10
Forest				X
Olive grove	X			
Potato		X		
Sugarbeet		X		
Sunflower	X	X	X	
Sorghum	X			
Corn	X	X		
Colza			X	
Alfalfa	X			
Dry wheat	X			
Bare soil	X			

parameter appears to be important since it is correlated with the dimensions of main stem, secondary stems, and leaves. These parameters have a remarkable influence on the radar signature. The following subdivision has been applied:

— low N: forest, olive grove;
— intermediate N: potato, sugarbeet, sunflower, sorghum, early stage corn;
— high N: colza, wheat, alfalfa.

Within "intermediate N" species, a further subdivision has been applied between potato, characterized by an extended ramification, and the other species, characterized by few wide leaves.

- Further subdivision has been applied on the basis of the biomass. Forests (high biomass) are separated by olive groves (low biomass). Within "intermediate N" crops, two classes have been defined, corresponding to biomass values higher or lower than 2 kg/m^2. Finally, colza, which showed high biomass values at the time of the flights (>4 kg/m^2), has been separated from alfalfa and dry wheat, which at the time of the flights, showed values lower than $\sim$2 kg/m^2.

In synthesis, the scheme of Table I has been applied, in which the classes are indicated by dashed contours. According to this scheme, some species showing common geometrical properties have been grouped into the same class. This is the case of the classes grouping early stage wide leaf (corn, sorghum, sunflower) and developed wide leaf (sunflower, sugarbeet).

Actually, there is a geometrical difference between sunflower (high vertical main stems) and sugarbeet (no vertical stems). However, both experimental data and model simulations indicate that this difference produces negligible effects on those radar signatures ($\sigma^{\circ}_{\mathrm{LHV}}$, $\sigma^{\circ}_{\mathrm{CRR}} - \sigma^{\circ}_{\mathrm{CRL}}$) that are fundamental to classify wide leaf crops, as will be shown in Section III-D. As far as wheat is concerned, fields were relatively dry but, at C-band, produced scattering effects appreciably different than those of bare soils. Therefore, separation between bare soils and dry wheat fields is feasible. This result finds explanation in the high sensitivity of high frequencies (C-band) to vegetation, even if not fresh. On the other hand, wheat signatures were rather similar to those of alfalfa, in spite of differences in the moisture content. This is due to an important common property of the two plants, i.e., the presence of several small stems per unit area. To discriminate between alfalfa and wheat, multitemporal data would have to be available.

According to the previous considerations, the following classes have been finally defined:

- bare soil (surface scattering);
- senescent corn (large vertical stems, partial defoliation, dihedral effects);
- forest (low N, high biomass);
- olive grove (low N, low biomass);
- potato (intermediate N with ramification, high biomass);
- developed sunflower and sugarbeet (intermediate N and wide leaf, high biomass);
- early stage sunflower, corn and sorghum (intermediate N and wide leaf, low biomass);
- colza (high N and small stems, high biomass);
- alfalfa and drying wheat (high N and small stems, low biomass).

The subdivision indicated above is based on geometrical and biophysical differences among the nine classes. As will be shown later, these differences produce marked effects at some combinations of frequency and polarization. These effects may be explained by model simulations. In this way, reliability is guaranteed to the separations experimentally observed in the two sites.

C. The Model

For most of the classes defined in the previous section, model simulations have been carried out, aimed at demonstrating that one (or more) AIRSAR features allow separability of that class from the others, because of some specific properties of its radar signature. The polarimetric vegetation model developed at Tor Vergata University has been used. Its simulation results were compared in the past with several experimental data.

The model describes vegetation as an ensemble of discrete disc-shaped and cylinder-shaped dielectric scatterers, representing vegetation elements, overlying a homogeneous half-space with rough interface, representing the soil. Also vertical dielectric elements, simulating tree trunks or agricultural main stalks, may be included. Soil geometrical properties are represented by statistical parameters, i.e., surface height standard deviation and correlation length; soil permittivity is related to volumetric moisture content. Both the soil surface and the vegetation canopy are assumed to be symmetrical in azimuth. The model is based on the radiative transfer theory and can include multiple scattering effects. Moreover, it is fully polarimetric since the scattering behavior of the elements is described by a 4×4 Stokes matrix. Details about the model and comparisons with previous experimental data are given in [4], [5], and [14].

In this paper, the model has simulated the polarimetric properties of each vegetation type. Simulations have been carried out for various values of the canopy height, ranging from zero to a typical maximum value. Some input data, such as stem and leaf dimensions, biomass, etc., have been related to the canopy height using empirical relationships based on ground measurements carried out during recent campaigns [8], [10], [15]. In this way, the effects of growing stage may be appreciated. Other input data, which showed small variations, such as plant moisture content and leaf thickness, have been assumed to be constant, and their values have been selected on the basis of average ground data at the time of the flights.

To classify ramified structures, such as forest, olive grove, and potato, the HV-polarization (at P- and L-band) has been used. Trunks and main stems may be considered as dihedral vertical elements, and well-established theories indicate that they produce negligible effects at HV-polarization with respect to inclined cylinders (branches or secondary stems) [2], [16]. Therefore, the backscatter of ramified vegetation species has been computed taking simply into account contributions from ensembles of equal dielectric cylinders of various dimensions, randomly oriented. For the above-mentioned reasons, the polarimetric properties relevant to our objective are represented with acceptable accuracy.

For wide leaf crops, all scattering sources have been considered, i.e., soil, vertical stems, leaves, and secondary stems (or petioles). Input data are valid (on average) for corn, sunflower, and sorghum fields. Sugarbeet fields have not vertical stems. However, the effect of vertical stems is negligible at the radar configurations useful for these crops ($\sigma^\circ_{\mathrm{LHV}}$ and $\sigma^\circ_{\mathrm{CRR}} - \sigma^\circ_{\mathrm{CRL}}$). The following input data have been used for wide leaf:

- $N = 8$ m^{-2};
- height $=$ 0–200 cm;
- stalk diameter $=$ 0–2.75 cm;
- LAI $=$ 0–6;
- leaf thickness $=$ 0.025 cm;
- inclined stem diameter $=$ 0–0.5 cm;
- inclined stem length $=$ 0–37.5 cm;
- biomass (linearly increasing with height) $=$ 0–6 kg/m^2;
- plant moisture content $=$ 85%.

For senescent and partially defoliated corn, a similar scheme has been adopted, but with a moisture content of 75%, an LAI of two, and a maximum height of 250 cm.

Colza and alfalfa were dominated by small stems, while leaves were very small or absent. The following input data have been used to simulate, on average, the behavior of these crops:

- N variable between 500 m^{-2} (lower canopies) and 100 m^{-2} (higher canopies);
- height $=$ 0–150 cm;
- stalk diameter $=$ 0–1.5 cm;
- inclined cylinder diameter $=$ 0–0.35 cm;
- inclined cylinder length $=$ 0–8.75 cm;
- biomass (linearly increasing with height) $=$ 0–6 kg/m^2;
- plant moisture content $=$ 80%.

The dry wheat fields of Montespertoli showed some properties (density and dimensions of stems, absence of leaves) compatible with previous data, while other properties were not (lower moisture, lower ramification). However, experimental wheat signatures are close to alfalfa ones, at least for the considered frequencies and polarizations (see Section III-D).

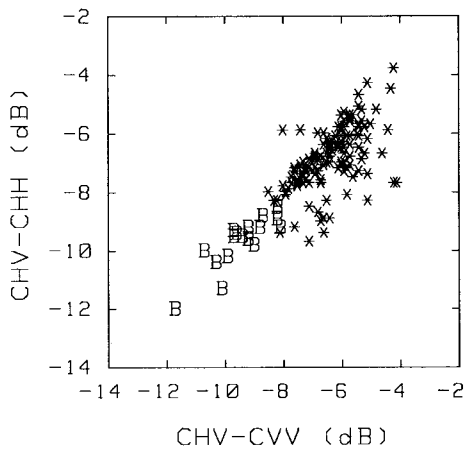

Fig. 1. $\sigma^\circ_{\mathrm{CHV}} - \sigma^\circ_{\mathrm{CHH}}$ versus $\sigma^\circ_{\mathrm{CHV}} - \sigma^\circ_{\mathrm{CVV}}$ for all experimental data (B: bare soil; $*$: other fields).

For all structures, leaves (simulated by discs) and small cylinders have been assumed to be randomly oriented. For soil, an average standard deviation of 1 cm has been assumed, while the moisture content has been set equal to 10% for crops mainly present at Montespertoli and to 20% for crops mainly present at Flevoland.

III. Results

Experimental data and model simulations obtained for the AIRSAR radar features (i.e., combination of frequency and polarization) that appear to be powerful in the discrimination of each of the nine classes are shown in this section. Experimental data are presented in the form of scatterplots of backscatter coefficients averaged among pixels belonging to a given field. The data are given in decibels.

In the following, the classes will be listed in the order selected on the basis of the class definition described in Section II-B and an elimination approach is adopted: once a class is assumed to have been identified, its samples are removed in the forthcoming scatterplots.

A. Bare Soil

Well-established theories indicate that, in bare soils, where surface scattering is dominant, the backscatter is less depolarized than in presence of vegetation, where volume scattering is important [16]. This property may be used to discriminate bare soils from vegetated fields. To this aim, the use of higher frequencies is advantageous since volume scattering effects may be appreciated even in the case of short (or relatively dry) vegetation. Fig. 1 shows a scatter plot of the difference $\sigma^\circ_{\mathrm{CHV}} - \sigma^\circ_{\mathrm{CHH}}$ versus $\sigma^\circ_{\mathrm{CHV}} - \sigma^\circ_{\mathrm{CVV}}$. The experimental data plotted in the figure confirm the theory, indicating that the scattering due to bare soils is less depolarized (lower values of $\sigma^\circ_{\mathrm{CHV}} - \sigma^\circ_{\mathrm{CHH}}$ and $\sigma^\circ_{\mathrm{CHV}} - \sigma^\circ_{\mathrm{CVV}}$) than that of vegetated fields. In general, the discrimination is achieved in spite of variations

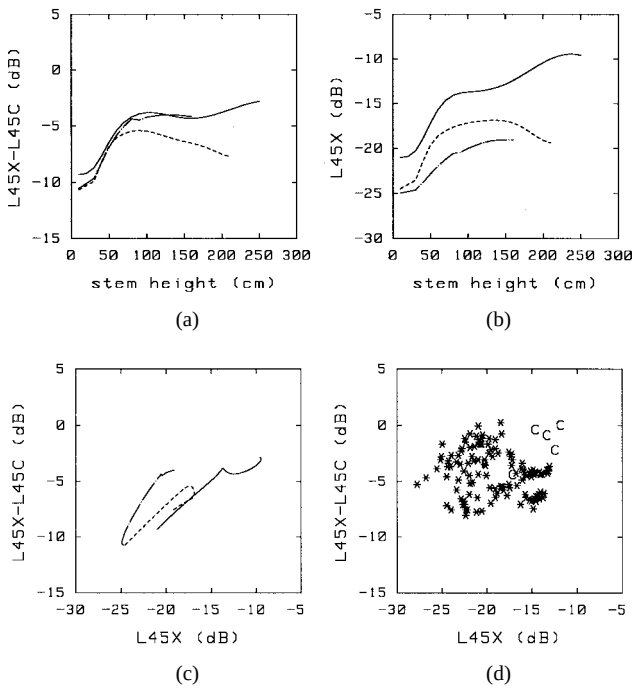

Fig. 2. (a)–(c) Simulated data (continuous lines: senescent corn; dashed lines: wide leaf; dash-dotted lines: small stem). (d) Experimental data (C: senescent corn; $*$: other fields).

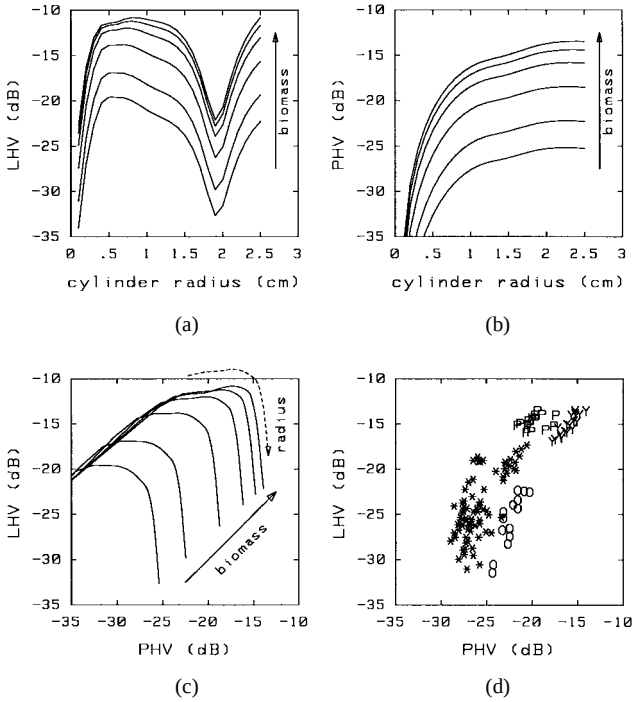

Fig. 3. (a)–(c) Simulated data for randomly oriented equal cylinders. (d) Experimental data (Y: forest; P: potato; O: olive grove; $*$: other fields).

in soil moisture and soil roughness. It has been checked that the less-discriminable bare soil samples are rough and dry soils, where some volume scattering could be present, due to air bubbles.

B. Senescent Corn

Ground data collected at Flevoland indicate that corn fields of that site were characterized by the dominance of vertical stalks with height $\cong$200 cm, diameter $=$ 2–3 cm and low moisture (70–80%). In some cases, leaves had severely been damaged by a hailstorm.

A discriminant property of these corn fields is the high depolarization that vertical stems introduce when the incoming wave is linearly polarized with an orientation angle (as defined in [16]) $\psi = 45°$. The effect is particularly evident at L-band; we have verified that it is weaker at P-band, while it is quenched by the top canopy attenuation at C-band. Fig. 2(a) and (b) show the simulated trends of $\sigma^{\circ}_{\mathrm{L45X}} - \sigma^{\circ}_{\mathrm{L45C}}$ and $\sigma^{\circ}_{\mathrm{L45X}}$ as a function of stalk height. Corn fields had $\mathrm{LAI} = 2$ and a moisture content of 75%. When increasing height, high values of both $\sigma^{\circ}_{\mathrm{L45X}}$ and $\sigma^{\circ}_{\mathrm{L45X}} - \sigma^{\circ}_{\mathrm{L45C}}$ are achieved since the double bounce effect is high and suffers low attenuation. It may be observed that lower values of both $\sigma^{\circ}_{\mathrm{L45X}}$ and $\sigma^{\circ}_{\mathrm{L45X}} - \sigma^{\circ}_{\mathrm{L45C}}$ are achieved for wide leaf and small stem crops, respectively. The same has been verified for potato and arboreous vegetation. Fig. 2(c) shows simulated data of $\sigma^{\circ}_{\mathrm{L45X}} - \sigma^{\circ}_{\mathrm{L45C}}$ versus those of $\sigma^{\circ}_{\mathrm{L45X}}$, while Fig. 2(d) shows the corresponding experimental scatter plot. In agreement with simulation results, Fig. 2(d) shows that, for both polarimetric parameters, most of the corn fields (four out of five) achieve values clearly higher than those of all the other samples.

C. Forest, Olive Grove, and Potato

Forests, olive groves and potato fields show differences in their geometrical structures, but have in common the presence of extended ramifications, i.e., branches or secondary stems. In forests, which are very dense at Montespertoli site, ramifications show various dimensions, ranging from those of small twigs to those of larger branches (i.e., 5–6 cm of diameter). Olive groves are sparse, characterized by large branches and trunks that appreciably depart from vertical position, while the density of small branches is often reduced by pruning techniques. Flevoland potato fields are dense; although no detailed measurements of secondary stem dimensions are available, it may be inferred, by visual inspections over photos, that those dimensions are, on average, smaller than those of forests and olive branches. Nevertheless, they are greater than those of the stems of other agricultural crops, like alfalfa.

It is well established that inclined cylinders generate high depolarization effects, with $\sigma^{\circ}_{\mathrm{HV}}$ much higher than that produced by surfaces or vertical cylinders [2], [16]. The wavelength at which these effects are more evident depends on the cylinder dimensions. A layer of equal randomly oriented dielectric cylinders has been considered, and the $\sigma^{\circ}_{\mathrm{HV}}$ at P- and L-band has been computed as a function of cylinder radius under the following assumptions: cylinder radius ranging from 0.1 to 2.5 cm, cylinder length $=$ 150 times the cylinder radius, plant moisture content ranging from 60 (largest cylinders) to 90% (smallest cylinders).

Fig. 3(a) and (b) show the trends of $\sigma^{\circ}_{\mathrm{LHV}}$ and $\sigma^{\circ}_{\mathrm{PHV}}$, respectively, for canopies of randomly oriented equal cylinders as a function of cylinder radius for various values of branch biomass in the range 0.1–2 kg/m^2. In the considered range

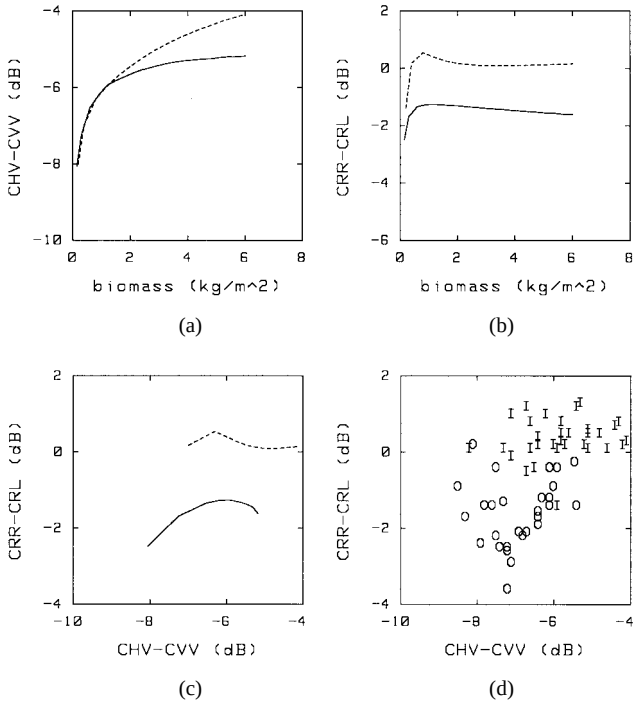

Fig. 4. (a)–(c) Simulated data (continuous lines: wide leaf; dashed lines: small stem). (d) Experimental data (O: wide leaf; I: small stem).

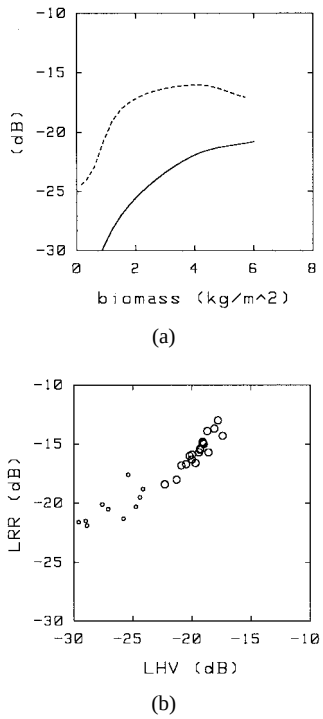

Fig. 5. (a) Simulated data for wide leaf (continuous line: $\sigma^{\circ}_{\mathrm{LHV}}$; dashed line: $\sigma^{\circ}_{\mathrm{LRR}}$). (b) Experimental data (large circles: biomass >2 kg/m^2; small circles: biomass <2 kg/m^2).

of radius values, which is realistic for stems and branches, a monotonic increasing trend is observed at P-band, while a minimum, which is typical of cylinder scattering [17], is observed at L-band and at $\sim$2 cm. Fig. 3(c) shows simulated values of $\sigma^{\circ}_{\mathrm{PHV}}$ versus $\sigma^{\circ}_{\mathrm{LHV}}$, while Fig. 3(d) shows a scatterplot of the corresponding field averages. Forest, olive groves, and potato classes are well discriminable in this figure. A comparison between the results of Fig. 3(a)–(c) and those of Fig. 3(d) suggests the following interpretation. The dense Montespertoli forests contain several branches whose dimensions are spread in a wide range, so that they produce high HV backscatter at both P- and L-band. Potato secondary stems have small radii, so that $\sigma^{\circ}_{\mathrm{LHV}}$ is higher than $\sigma^{\circ}_{\mathrm{PHV}}$. Olive groves are sparse, with few branches (and inclined trunks) per m^2 and their dimensions are such to produce a $\sigma^{\circ}_{\mathrm{PHV}}$ higher than $\sigma^{\circ}_{\mathrm{LHV}}$. In Fig. 3(d), the samples of all the other fields are located within a "cloud." However, further separations are achievable using C-band multipolarization data, as will be shown in the forthcoming section.

D. Other Agricultural Fields

Crops with small cylindrical elements, like colza, wheat, and alfalfa, may be distinguished by the other kinds of fields, i.e., wide leaf crops. Well-established theories [16] indicate that, when volume scattering dominates, both $\sigma^{\circ}_{\mathrm{HV}}$ and $\sigma^{\circ}_{\mathrm{RR}}$ are higher than when surface scattering dominates. Our simulations show that an appreciable difference is also noted when cylinder scattering is compared with disc scattering, particularly at circular polarization.

Fig. 4(a) and (b) show, respectively, the simulated values of the differences $\sigma^{\circ}_{\mathrm{CHV}} - \sigma^{\circ}_{\mathrm{CVV}}$ and $\sigma^{\circ}_{\mathrm{CRR}} - \sigma^{\circ}_{\mathrm{CRL}}$ for wide leaf

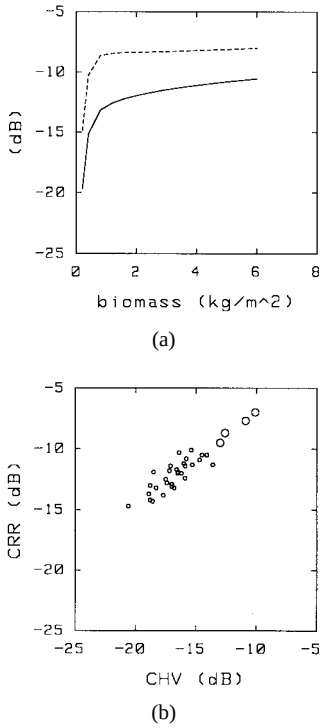

Fig. 6. (a) Simulated data for small stem (continuous line: $\sigma^{\circ}_{\mathrm{CRR}}$; dashed line: $\sigma^{\circ}_{\mathrm{CHV}}$). (b) Experimental data [large circles: biomass >4 kg/m^2 (colza); small circles: biomass <2 kg/m^2 (dry wheat, alfalfa)].

crops (continuous lines) and small stem crops (dashed lines) as a function of biomass. For high biomass, both differences are higher for small stem than for wide leaf. However, the figure indicates that a better discrimination, appreciable even at low

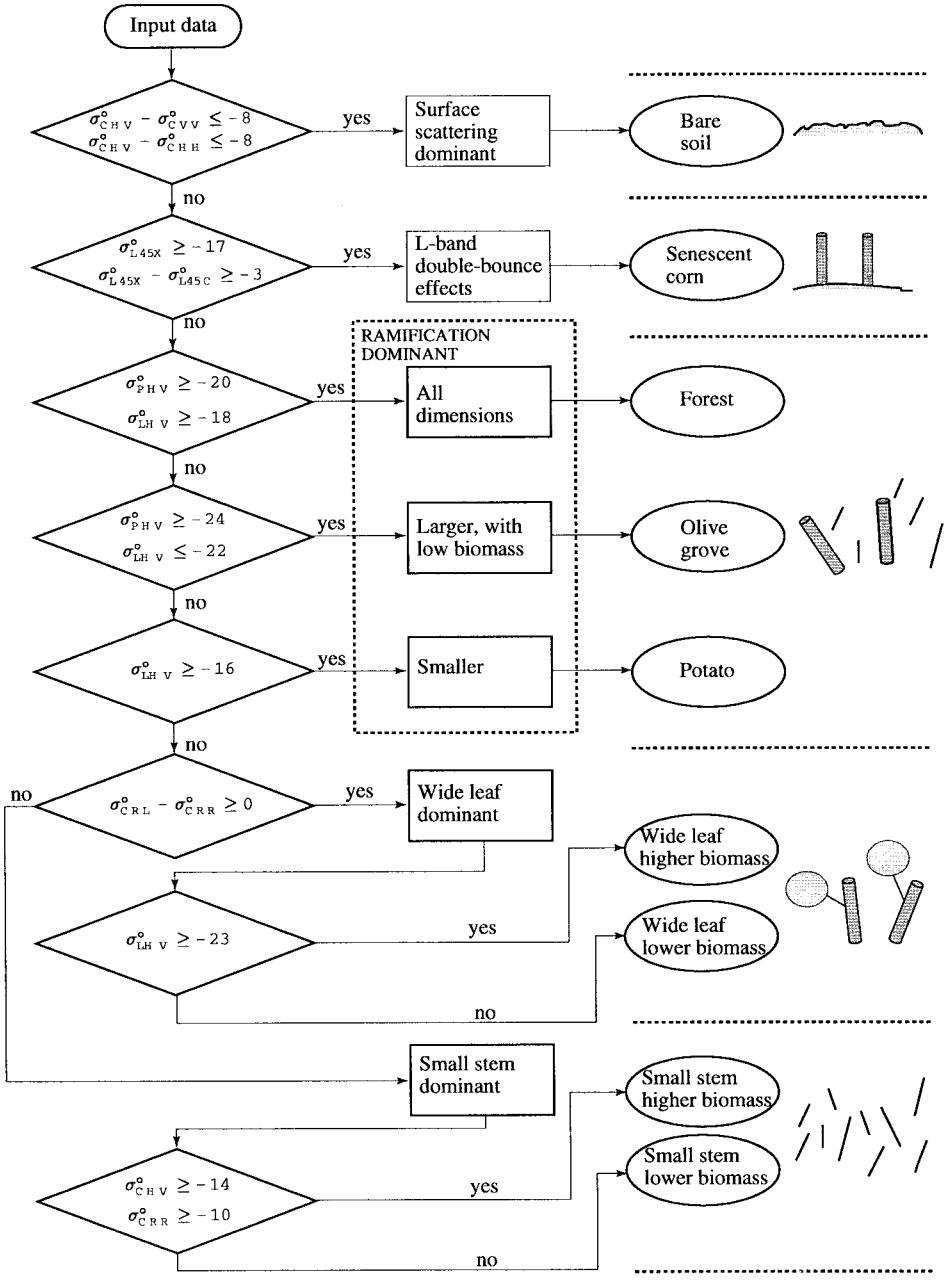

Fig. 7. Block diagram of the classification algorithm.

biomass, may be achieved using the $\sigma^{\circ}_{CRR} - \sigma^{\circ}_{CRL}$ difference. Fig. 4(c) shows the modeled $\sigma^{\circ}_{CRR} - \sigma^{\circ}_{CRL}$ versus $\sigma^{\circ}_{CHV} - \sigma^{\circ}_{CVV}$, while Fig. 4(d) shows the corresponding experimental field averages, generally confirming the difference between the two crop groups.

Finer subdivisions may be established on the basis of biomass. For wide leaf crops, Fig. 5(a) shows σ°_{LHV} and σ°_{LRR} as a function of biomass. An increasing trend is evident for both parameters and the best dynamic range is noted in σ°_{LHV}. Fig. 5(b) shows a scatterplot of σ°_{LRR} versus σ°_{LHV}, indicating that both parameters are able to discriminate between crops with biomass <2 kg/m^2 and those with biomass >2 kg/m^2; σ°_{LHV} shows the best dynamic range also in the experimental data.

For small stem crops, such as colza and alfalfa, Fig. 6(a) shows that the model predicts a significant increase of σ°_{CHV} and σ°_{CRR} when the biomass increases between zero and $\sim$2 kg/m^2. The experimental data of Fig. 6(b) show that both σ°_{CHV} and σ°_{CRR} are efficient in discriminating between colza fields, characterized by biomass values higher than $\sim$4 kg/m^2 and alfalfa fields, for which biomass was variable, but in any case lower than $\sim$2 kg/m^2, at the time of AIRSAR flights. Wheat samples showed values similar to alfalfa ones. It must be stressed that the radar surveys took place in summertime when wheat fields were dry. Therefore, these results cannot be simply extended to predict the springtime behavior of wheat since fresh leaves and fresh vertical stalks produce different effects and must be modeled with different assumptions.

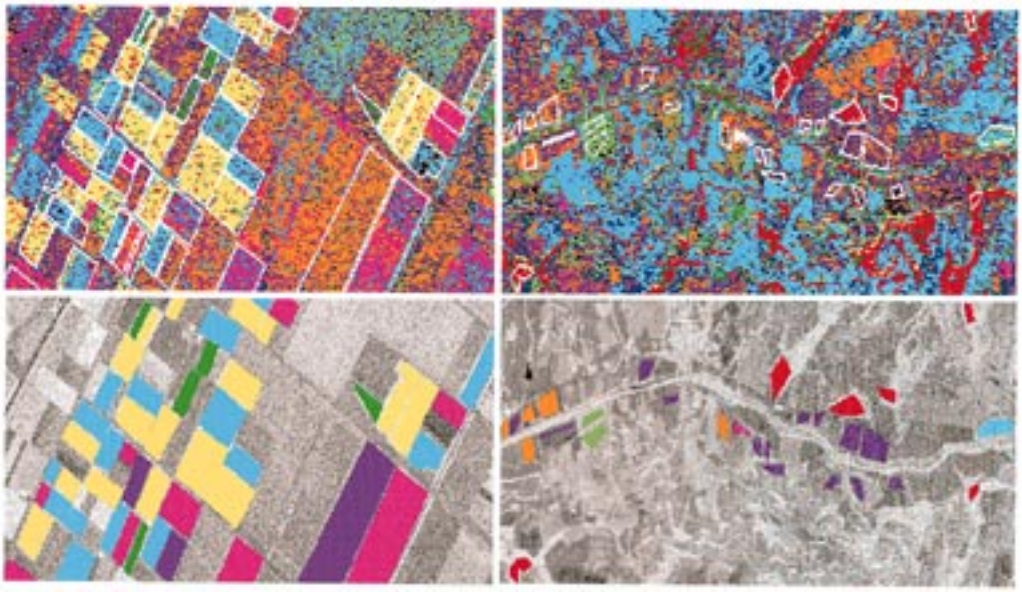

Fig. 8. Upper: classified images of Flevoland site (left) and Montespertoli site (June 22 flight) (right). Lower: corresponding ground truth (the background is an L-band HV-polarization image). Magenta: bare soil; dark green: senescent corn; red: forest; blue: olive grove; yellow: potato; cyan: wide leaf with higher biomass; orange: wide leaf with lower biomass; green: small stem with higher biomass; violet: small stem with lower biomass; black: unclassified.

IV. Applications

On the basis of the results described in Section III, it appears that, for each of the nine classes defined in the present paper, there is at least one multifrequency polarimetric radar configuration able to discriminate that class. This possibility is related to specific geometrical and/or biophysical properties of vegetation belonging to that class and is confirmed by model simulations.

To investigate the potential applications of these results, a simple hierarchical parallelepiped classification algorithm [18] has been developed. The basic structure is similar to that proposed in [13] for the Montespertoli data acquired at an incidence angle of 35°. Some modifications have been introduced, and further validations come from inclusion of MAESTRO-1 data and comparisons with model simulations. The adopted scheme, which follows from the results of Section III, is shown in Fig. 7. When the algorithm is applied to the fields observed during MAESTRO-1 and MAC-Europe flights, the following percentages of correct classification are obtained: 70.5% at 3×3 pixel average level, 90.5% at per-field average level. The previous accuracies were evaluated using all of the fields with ground truth. We have noted that the algorithm leads to good discrimination results in the case of developed vegetation when the scattering differences associated to different plant geometries are fully evident. Most of the ambiguities are due to confusion among bare soils and the two kinds of low biomass fields; also, the effects of senescence in corn fields are not always evident, especially when the analysis is carried out at 3×3 pixel level. To estimate these effects, we have repeated the computations after reducing the number of the classes, i.e., tolerating the confusion between bare soils and low biomass fields, and that between senescent corn and developed wide leaf. For the sic classes obtained in this way, the percentage of correct classification increases to 83.5% in the 3×3 pixel case and to 94.8% in the per-field case.

The classified images of Flevoland and Montespertoli (June 22 flight) sites are shown in Fig. 8, with the corresponding ground truth for the selected polygons. The Flevoland site is flat, with large rectangular fields. On the contrary, the Montespertoli site is characterized by small fields with irregular borders; outside the selected fields, the site is hilly and even more irregular, as the SAR image confirms. However, when only the selected polygons are considered, the classification algorithm achieves comparable accuracy results between one site and the other. For both sites, the images confirm that most of the classification problems are due to confusion between the two classes characterized by low biomass.

It must be reminded that the study is based on airborne surveys of agricultural areas carried out in summer time by a three-frequency polarimetric SAR. The suggested classification scheme could be seen as a preliminary guideline when similar remote-sensing data (i.e., multifrequency, multipolarization, single flight) are available. In that case, after testing and refining over different sites, a reliable tool could be achieved. Of course, the proposed scheme cannot be used for spaceborne remote-sensing systems, where neither multifrequency nor polarimetry are at present available. However, the results of this research give indications about the classification potential of single-frequency bands. For example, C-band (available with three polarizations on the future ENVISAT) is useful to discriminate between bare soils and fields with vegetation (even if short or moderately dry) and to classify among some broad crop classes and/or biomass levels. Other discriminations do not appear to be feasible with a single flight and the single C-band, but advantages may be taken by multitemporality. For example, forests could be identified using HV-polarization in winter time overpasses.

V. Conclusions

The classification capability of multifrequency polarimetric SAR has been investigated using experimental data collected

over two European sites and model simulations. The results reported in this paper indicate reliable criteria of class selection since model validations give sound explanations to the different polarimetric behaviors of the selected classes. The research has mostly been carried out at field average level, but this may have some operational benefits if accompanied with preliminary application of edge detection techniques [19]; the synergy with optical data may facilitate this operation. We have also shown that the classes may be defined both on the basis of the crop type and on the basis of the crop development (biomass). When applied to vegetation data bases larger than that at present available to us, this approach could lead to a solution of the classification problem that includes a stepwise solution of the inversion problem.

Of course, the use of advanced statistical image processing techniques will lead to more directly applicable results. However, the results of this paper could give some benefits to remote-sensing applications. Validations and eventual refinements based over data acquired in other campaigns may give greater reliability to classification rules. Further benefits could be derived by combined use of optical data. Moreover, the model may be used to investigate the classification ability of the future satellite SAR systems, which are neither polarimetric nor multifrequency, but offer important advantages associated to multitemporality.

ACKNOWLEDGMENT

Information about the Flevoland site has been made available by the University of Wageningen (NL).

REFERENCES

[1] M. C. Dobson, L. E. Pierce, and F. T. Ulaby, "Knowledge-based landcover classification using ERS-1/JERS-1 SAR composites," *IEEE Trans. Geosci. Remote Sensing*, vol. 34, pp. 83–99, Jan. 1996.

[2] J. J. Van Zyl, "Unsupervised classification of scattering behavior using radar polarimetry data, " *IEEE Trans. Geosci. Remote Sensing*, vol. 27, pp. 36–45, Jan. 1989.

[3] A. Freeman, B. Chapman, and M. Alves, *MAPVEG Software User's Guide*, JPL Document D-11254, 1993.

[4] P. Ferrazzoli and L. Guerriero, "Radar sensitivity to tree geometry and woody volume: A model analysis," *IEEE Trans. Geosci. Remote Sensing*, vol. 33, pp. 360–371, Mar. 1995.

[5] M. Bracaglia, P. Ferrazzoli, and L. Guerriero, "A fully polarimetric multiple scattering model for crops," *Remote Sens. Environ.*, vol. 54, pp. 170–179, 1995.

[6] D. H. Held, W. E. Brown, A. Freeman, J. D. Klein, H. Zebker, T. Sato, Q. Nguyen, and Y. Lou, "The NASA/JPL multifrequency multipolarization airborne SAR system," in *Proc. Int. Geosci. Remote Sensing Symp.*, Edinburgh, U.K., 1988, pp. 345–349.

[7] P. de Matthaeis, G. Schiavon, and D. Solimini, "Effect of scattering mechanisms on polarimetric features of crops and trees," *Int. J. Remote Sensing*, vol. 15, pp. 2917–2930, 1994.

[8] S. Baronti, F. Del Frate, P. Ferrazzoli, S. Paloscia, P. Pampaloni, and G. Schiavon, "SAR polarimetric features of agricultural areas," *Int. J. Remote Sensing*, vol. 16, pp. 2639–2656, 1995.

[9] P. N. Churchill and E. P. W. Attema, "The MAESTRO-1 European airborne polarimetric synthetic aperture radar campaign," *Int. J. Remote Sensing*, vol. 15, pp. 2707–2718, 1994.

[10] W. J. Droesen, D. H. Hoekman, H. J. C. Van Leeuwen, J. J. Van der Sanden, S. A. M. Bouman, D. Uenk, M. A. M. Vissers, and G. G. Lemoine, "MAESTRO 89 ground data collection Hosterwold/Speulderbos/Flevoland (NL)," Wageningen Agricultural Univ., Tech. Rep., 1990.

[11] G. G. Lemoine, G. F. de Grandi, and A. J. Sieber, "Polarimetric contrast classification of agricultural fields using MAESTRO-1 AIRSAR data," *Int. J. Remote Sensing*, vol. 15, pp. 2851–2870, 1994.

[12] D. E. Wickland, R. E. Murphy, and A. C. Janetos, "Overview of MAC Europe'91 campaign and NASA airborne imaging spectrometry and radar programs, " in *Proc. 25th ERIM Int. Symp. Remote Sensing Global Environ. Change*, Graz, Austria, 1993, pp. I66–I75.

[13] P. Ferrazzoli, G. Schiavon, D. Solimini, S. Paloscia, P. Pampaloni, and S. Sigismondi, "The potential of multifrequency polarimetric SAR in assessing agricultural and arboreous biomass," *IEEE Trans. Geosci. Remote Sensing*, vol. 35, pp. 5–17, Jan. 1997.

[14] P. Ferrazzoli and L. Guerriero, "Interpretation and model analysis of MAESTRO-1 Flevoland data," *Int. J. Remote Sensing*, vol. 15, pp. 2901–2915, 1994.

[15] P. Ferrazzoli, S. Paloscia, P. Pampaloni, G. Schiavon, D. Solimini, and P. Coppo, "Sensitivity of microwave measurements to vegetation biomass and soil moisture content: A case study," *IEEE Trans. Geosci. Remote Sensing*, vol. 30, pp. 750–756, May 1992.

[16] F. T. Ulaby and C. Elachi, Eds., *Radar Polarimetry for Geoscience Applications.* Norwood, MA: Artech House, 1990.

[17] G. T. Ruck, Ed., *Radar Cross Section Handbook.* New York: Plenum, 1970.

[18] T. M. Lillesand and R. W. Kiefer, *Remote Sensing and Image Interpretation.* New York: Wiley, 1987.

[19] R. Touzi, A. Lopes, and P. Bousquet, "A statistical and geometrical edge detector for SAR images," *IEEE Trans. Geosci. Remote Sensing*, vol. GE-26, pp. 764–773, May 1988.

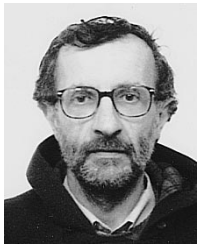

Paolo Ferrazzoli (M'95) received a degree from the University of Rome "La Sapienza," Rome, Italy, in 1972.

He joined Telespazio s.p.a. in 1974, where he was mainly active in the fields of antennas, slant-path propagation, and advanced satellite telecommunication systems. In 1984, he joined "Tor Vergata" University, Rome, where he is presently teaching microwaves. His research concerns propagation and microwave remote sensing of vegetated terrains, with particular emphasis on electromagnetic modeling. He has been involved in international experimental remote-sensing campaigns, such as AGRISAR, AGRISCATT, MAESTRO-1, MAC-Europe, and SIR-C/X-SAR.

Leila Guerriero received the Laurea degree in physics in 1986 and the Ph.D. degree in electromagnetism in 1991.

She has been a Permanent Researcher at "Tor Vergata" University, Rome, Italy, since 1994, where she is mainly concerned with modeling microwave backscattering and emissivity from agricultural and forested areas. In 1988, she was involved in a cooperation between the Jet Propulsion Laboratory, Pasadena, CA, and the Italian National Research Council for investigations on geophysical applications of imaging spectrometry in infrared and visible remote sensing.

Giovanni Schiavon received the Laurea degree in electronic engineering from the University of Rome "La Sapienza," Rome, Italy, in 1982.

He has been with the University of Rome "Tor Vergata" since 1984, where he teaches a course on remote sensing. His research activity has been concerned with propagation, remote sensing, and millimeter waves. He has been involved in the international remote-sensing projects AGRISAR, AGRISCATT, MAESTRO-1, MAC-Europe, and SIR-C/X-SAR.